

Alma Mater Studiorum Università di Bologna  
Archivio istituzionale della ricerca

Rapid exhumation since at least 13 Ma in the Himalaya recorded by detrital apatite fission-track dating of Bengal fan (IODP Expedition 354) and modern Himalayan river sediments

This is the final peer-reviewed author's accepted manuscript (postprint) of the following publication:

*Published Version:*

Huyghe, P., Bernet, M., Galy, A., Naylor, M., Cruz, J., Gyawali, B.R., et al. (2020). Rapid exhumation since at least 13 Ma in the Himalaya recorded by detrital apatite fission-track dating of Bengal fan (IODP Expedition 354) and modern Himalayan river sediments. EARTH AND PLANETARY SCIENCE LETTERS, 534, 1-14 [10.1016/j.epsl.2020.116078].

*Availability:*

This version is available at: <https://hdl.handle.net/11585/961801> since: 2024-10-10

*Published:*

DOI: <http://doi.org/10.1016/j.epsl.2020.116078>

*Terms of use:*

Some rights reserved. The terms and conditions for the reuse of this version of the manuscript are specified in the publishing policy. For all terms of use and more information see the publisher's website.

This item was downloaded from IRIS Università di Bologna (<https://cris.unibo.it/>).  
When citing, please refer to the published version.

(Article begins on next page)

**Rapid exhumation since at least 13 Ma in the Himalaya recorded by detrital  
apatite fission-track dating of Bengal fan (IODP Expedition 354) and  
modern Himalayan river sediments**

**P. Huyghe<sup>a,\*</sup>, M. Bernet<sup>a</sup>, A. Galy<sup>b</sup>, M. Naylor<sup>c</sup>, J. Cruz<sup>d</sup>, B.R. Gyawali<sup>e</sup>, L. Gemignani<sup>f</sup>,  
J.L. Mugnier<sup>g</sup>**

*<sup>a</sup>ISTerre, Université Grenoble Alpes, CNRS, 38058 Grenoble, France*

*<sup>b</sup>CRPG, Université de Lorraine, 54500 Vandœuvre-Lès-Nancy, France*

*<sup>c</sup>University of Edinburgh, School of Geosciences, Edinburgh, UK*

*<sup>d</sup>Florida State University, Earth, Ocean & Atmospheric Sciences, Tallahassee, FL, USA*

*<sup>e</sup>Department of Physics (Geology), Central Campus of Technology Tribhuvan University,  
Nepal*

*<sup>f</sup>Department of Earth Sciences, Vrije Universiteit Amsterdam, 1081 HV Amsterdam, the  
Netherlands*

*<sup>g</sup>ISTerre, Université Savoie Mont Blanc, CNRS, 38058 Grenoble, France*

*\* Corresponding author: [pascale.huyghe@univ-grenoble-alpes.fr](mailto:pascale.huyghe@univ-grenoble-alpes.fr)*

**Keywords:** Bengal fan, Himalayan rivers, Siwaliks, detrital apatite fission-track data, lag  
time, exhumation, erosion, threshold hillslope

## Abstract

Apatite fission-track analysis of middle Bengal fan sediments (IODP expedition 354) and modern Himalayan river sediments shows that most of the detrital apatites are very young compared to their depositional ages, independent of their uranium content. Bengal fan apatites display an average central age lag time as short as  $2.26 \pm 1.6$  Myr since at least  $\sim 13$  Ma. Such lag times reflect a mean exhumation rate on the order of at least 1-3 km/Myr. The occurrence of detrital apatites with relatively short AFT lag times since at least 13 Ma indicates that there have always been areas of rapid erosional exhumation, supplying detrital apatites to the fluvial system and delivering them to the paleo-Ganges and/or –Brahmaputra plains and finally to the Bengal fan. It also supports that temporary storage of detrital apatites in the floodplains or delta has always been negligible since at least 13 Ma. Comparison of the AFT data of the Bengal fan with those of the Central and Eastern proximal Neogene Himalayan foreland basin shows that both paleo-Ganga and –Brahmaputra catchments provided apatites with similar short lag time to the distal Bengal Fan basin.

In the modern drainage system of the Bengal fan, the apatites with young fission-track cooling ages are principally derived from areas where the topography has a sharp relief controlled by threshold hillslope processes and stream power resulting in landslide erosion as a coupled response to tectonic and fluvial forcing. By analogy with the modern erosion processes in the Himalayan range, we suggest that over the past 13 Ma, apatites were mainly derived from areas of sharp relief, where river stream power was high and hill slopes close to the threshold angle. As the exhumation signal is rather consistent since the late Miocene the detrital apatite fission-track data are either not sensitive enough to detect rapid climatically controlled changes in exhumation rates, or overall long-term erosion rates on the orogen scale are not strongly affected by climatic variations such as the variability of the Indian Summer Monsoon. Given the already rapid exhumation rates controlled by tectonics, the impact of climate

variability on surface erosion rates cannot be detected with our data, especially in the case of erosion processes dominated by threshold hillslope model.

## **1. Introduction**

Understanding the dynamics of convergent mountain building, the sequence of thrusting and rates of erosional exhumation are crucial for understanding crustal deformation and for studying the influence of sediment flux on ocean geochemistry or tectonic and climatic coupling. The rate at which rocks are exhumed by erosion and the derived sediment transported to adjacent sedimentary basins is at the centre of studying the relationship between tectonic and surface processes in orogenic mountain belts. Given the large volume of particulate materials delivered by the Ganges and Brahmaputra rivers to the Indian Ocean at least since the Late Eocene – Oligocene (Najman et al., 2008), the study of Himalayan mountain building is of prime interest (Fig. 1A). Geological field studies provide a valuable, but partial, record of Himalayan mountain building. The mineralogical, isotopic and thermochronological analysis of Neogene sedimentary rocks provide a complementary dataset that records the unroofing history of the Himalaya, either from the proximal Siwaliks foreland basin (e.g. DeCelles et al., 2001; Huyghe et al., 2001; Bernet et al., 2006; van der Beek et al. 2006, Chirouze et al., 2013), or the Bengal fan turbidite deposits at the ODP 116 and DSDP 218 sites (e.g. Corrigan and Crowley, 1990; Copeland and Harrison, 1990; Galy et al., 1996; Galy et al., 2010).

Thermochronology of detrital grains in modern rivers or ancient sediments allows estimating present-day or paleo-exhumation rates from the lag times between the apparent cooling age and the depositional age of the detrital material in the river, the foreland basin or on the submarine fan (e.g. Cervený et al., 1988). Using apatite fission-track (AFT) low-temperature

thermochronology, the exhumation record from the Siwalik foreland basin and modern river deposits is restricted to the period of the past ~7 Ma because post-depositional partial annealing of fission tracks in apatites affected AFT ages in deeply buried sedimentary rocks (van der Beek et al., 2006; Chirouze et al., 2013). The Bengal fan presents a thinner, more condensed, Neogene section, and therefore much less buried, which allows extending the exhumation back to the mid-Miocene (Corrigan and Crowley, 1990). Here we present AFT data of twenty-three new detrital samples from the <20 Ma record of the Bengal fan at 8°N in the Indian Ocean collected in 2015 during the IODP expedition 354 (Fig. 1A; France-Lanord et al., 2016). In addition, AFT data from six new modern river samples are also presented, together with published data from two other rivers in order to decipher the detrital record linked to the present-day Himalayan exhumation pattern (Fig. 1A).

In this paper, we show that detrital apatite with young fission-track ages and short lag times dominate the Bengal fan sediments back to at least 13 Ma, similar to the exhumation signal seen in the river sediments. This implies that fast exhumation, at least in some of the Himalayan hinterland domains existed since at least that time. By analogy with the modern system, we propose that erosion is mainly controlled by sharp relief, where river stream power was high and hill slopes close to the threshold angle. As the method that we use for the acquisition of the AFT in the Bengal Fan is similar to that used in the Siwalik foreland basin of Central and Eastern Himalaya, we compare the two exhumation records. Therefore, we suggest that source rocks from Central and Eastern Himalaya equally contributed to the AFT short lag time recorded in the Bengal Fan. Finally, we discuss the impact of climate variability on surface erosion rates.

## **2. Geological setting**

100        The collision between the Indian and Asian plates began during late Paleocene - early  
101        Eocene times along the Indus-Yarlung suture zone (IYSZ), which juxtaposes the pre-collision  
102        Indian passive margin sequence to the south with the Cretaceous-Paleogene Andean-type  
103        Asian Transhimalayan batholiths and ophiolites to the north (e.g. Hu et al., 2015). South of  
104        the IYSZ, the Main Himalayan Thrust (MHT) accommodated convergence (e.g. Bollinger et  
105        al., 2006 and references herein), generating the Himalayan structure that consists of four major  
106        lithotectonic units delimited by north-dipping faults branching off the basal MHT. From north  
107        to south, these faults are the South Tibetan detachment, which separates the Neoproterozoic to  
108        Eocene Tethyan Sedimentary Series from the high-grade metasedimentary rocks and granites  
109        of the Greater Himalayan sequence. The Main Central thrust separates the Greater Himalayan  
110        sequence rocks from low-grade metasedimentary rocks of the Lesser Himalayan sequence.  
111        The Lesser Himalayan thrust system places the Lesser Himalayan rocks over the Siwalik  
112        Group clastic rocks of the Neogene foreland basin, which in turn were thrust over the  
113        Ganges and Brahmaputra alluvial plains along the Main Frontal thrust. East and West of the  
114        Himalayan arc, the Namche Barwa and the Nanga Parbat syntaxes, respectively, constitute  
115        north-south trending antiformal structures exposing high-grade metamorphic rocks of Indian  
116        origin (e.g. Zeitler et al., 2001; Seward and Burg, 2008).

117        The long-term exhumation of the Himalayan range has already been recorded since  
118        ~12 Ma by low-temperature thermochronometers such as zircon fission track (ZFT) or white  
119        mica  $^{40}\text{Ar}$ - $^{39}\text{Ar}$  dating of detrital grains preserved in the Siwalik sediments of Western, Central  
120        and Eastern Himalaya (e.g. Cervený et al., 1988; Bernet et al., 2006; Szulc et al., 2006;  
121        Chirouze et al., 2013). From *in situ* thermochronological data, rapid exhumation is evidenced  
122        in localized areas (e.g. Blythe et al., 2007; Seward and Burg, 2008; Robert et al., 2011; Thiede  
123        & Ehlers, 2013). Different tectonic processes are inferred to control exhumation: 1) 20°-30°

north dipping mid-crustal ramps affecting the rather flat MHT and localized surface uplift of the hanging wall (e.g. Bollinger et al., 2006); 2) active thickening occurs within portions of the orogenic wedge (Whipple et al., 2016) and is partly related to 3) out-of-sequence steep faults merging the basal thrust system (e.g. Hodges et al., 2004). At deeper levels, the ductile behaviour of the crust also controls zones of localized exhumation (Vannay et al., 2004). It has been suggested that a major zone of exhumation existed at the leading edge of a channel flow (e.g. Godin et al., 2006) that also involved the brittle levels located above the exhumed deep levels (4 on Fig. 1B). The viscous behaviour of the deep level favours rock motion out of the convergence direction and rapid exhumation in the Himalayan syntaxes (Zeitler et al., 2001; 5 on Fig. 1B). Slab dynamics has also been inferred to control much of the tectonic deformation of the Himalayan orogenic wedge (Mugnier and Huyghe, 2006; Webb et al., 2017). As these different tectonic interpretations are still debated, most researchers agree that localized surface uplift and exhumation processes result in physiographic sharp increases of the Himalayan relief with mean elevations above 6000 m and increasing erosion rates (Burbank et al., 2003; Hodges et al., 2004; Elliott et al., 2016). In these zones and altitudes, the kinetics of weathering and soil development are thought to be far less important than the bedrock uplift rates and erosion occurs through landsliding, which increases nonlinearly until being equal to river incision (Larsen and Montgomery, 2012) and hillslope angles approaching the threshold angle (e.g. Burbank et al., 2003).

## *2.2. The modern Bengal Fan catchment*

The modern Ganges catchment includes the Himalayan lithotectonic units described above. The modern Brahmaputra watershed also encompasses units from the IYSZ and from the Transhimalayan batholiths. Indo-Burmese Range material and the Precambrian Indian basement of the Mikir Hills/Shillong Plateau and its Tertiary sedimentary cover may also

slightly contribute to the sediment load of the Brahmaputra River (Lupker et al., 2017 and references therein).

The modern Ganges and Brahmaputra catchments provide respectively about  $390 \pm 30 \times 10^6$  and  $400\text{--}1160 \times 10^6$  tons/yr of sediment to the Bengal Fan (Lupker et al., 2017 and references therein). Overall present-day erosion rates of 0.7 to 1.2 mm/yr and 1.0–1.1 mm/yr on the  $10^3\text{--}10^4$  years time scale for respectively the entire Tsangpo-Brahmaputra and Ganga catchments have been deduced from  $^{10}\text{Be}$  analyses of detrital quartz of river sands (Lupker et al., 2017). Such rates may differ from long-term average exhumation rates derived from detrital apatite or zircon fission track data. The Lesser and Greater Himalayan domains are locally exhumed with mean rates of about 1.8 mm/yr and up to 5 mm/yr, respectively, based on detrital AFT and ZFT data and *in situ* AFT (Bernet et al., 2006; van der Beek et al., 2006; Blythe et al., 2007; Thiede and Ehlers, 2013 and references therein). North of the IYSZ, the Transhimalayan batholiths had a very episodic history of erosion with some intervals with less than 0.3 mm/year and others exceeding 4 mm/year (Copeland et al., 1987) whereas the Namche Barwa syntaxis experiences exhumation at rates of up to 5–10 mm/yr (e.g. Seward and Burg, 2008). Therefore the exhumation of the Himalaya varies in time and space: fast exhumation rates only occur in some locations of the Himalaya (e.g. Thiede & Ehlers, 2013) and are then greater than the average erosion rates.

### 3. Sampling

The IODP Expedition 354 drilled the Bengal fan at  $8^\circ\text{N}$  (Fig. 1A). This study is based on the deepest sites (U1450) and (U1451) which reached ~ 800 m and ~1200 m below sea floor respectively (Table 1), recovering Quaternary to Paleogene turbidite and hemipelagic sediments (France-Lanord et al., 2016). The samples consist of siltstones and fine-grained sandstones, corresponding to the coarsest basal parts of thick turbidites, stratigraphically dated



by the micro- and nanno-fauna present in the intercalated hemipelagic deposits. Mineralogical and geochemical analyses showed that the turbidite material has very strong affinity to sand and silt of the modern Ganges and Brahmaputra rivers and are therefore relevant for reconstructing erosion and changes in Himalayan hinterland source areas (France-Lanord et al., 2016). For this study, we use the stratigraphic age model established by France-Lanord et al. (2016) from the mean age of the nannofossils, foraminifera and Chrons acquired onboard refined for the <1.9 Ma deposits by the magnetostratigraphic model of Reilly (2018). The uncertainty in the depositional > 1.9 Ma ages is taken as the difference between the mean age from France-Lanord et al. (2016) and the age of the youngest fauna considering that older fauna in turbidite horizons could be recycled from previously deposited sediments on the fan, resulting in a depositional age estimates that is too old.

In addition, eight modern river sand samples from the Ganges-Brahmaputra catchment have been used in this study, six new samples (Fig. 1A, Table 2), and published detrital AFT data of the Kameng and Rangit river samples were taken from Chirouze et al. (2013) and Abrahimi et al. (2016) respectively.

#### **4. Apatite Fission-Track analysis**

Apatite is an accessory mineral and only represents about one in every 1000 detrital grains in the Ganges and Brahmaputra sands (Garzanti et al., 2010), but it can be readily found in river and marine sediments, and the Bengal fan turbidites (Corrigan and Crowley, 1990). Even though the fraction is small for most samples sufficient apatite crystals were recovered for fission-track dating. We used the 80-160  $\mu\text{m}$  fraction of fine-grained sandstone for AFT analysis. Apatite grains were separated using standard heavy liquid and magnetic separation techniques. Apatite aliquots were mounted in epoxy, polished to expose internal crystal surfaces, and etched for 20 s at 21°C with 5.5 M  $\text{HNO}_3$ . All samples were covered with

198 muscovite mica sheets as external detectors and sent for neutron irradiation to the FRM II  
199 Research Reactor at the Technische Universität München in Garching, Germany. Apatite  
200 samples were irradiated together with IRMM540R dosimeter glasses (15 ppm U) and Durango  
201 and Fish Canyon Tuff age standards.

202       After irradiation the mica sheets of all samples and standards were etched for 18 min at  
203 21°C in 48% HF. All datable grains, including zero-track grains, within a mount were included  
204 in the analysis. Grains were selected for dating primarily on their orientation parallel to the c-  
205 axis and on the basis of the grain images in the mica detectors. The samples and standards  
206 were counted dry at 1250x magnification, using an Olympus BX51 optical microscope and the  
207 FTStage 4.04 system of Trevor Dimitru. The objective was to date up to 100 grains per  
208 sample, when that was possible, depending on available sample material and grain quality.

#### 210       *4.1 Track count statistics and zero-track grains*

211       The precision of AFT grain ages depends on track counting statistics. The more  
212 induced and spontaneous tracks can be counted, the smaller the individual grain age  
213 uncertainty becomes (Galbraith, 2005). As we used the external detector method for AFT  
214 dating in this study, one needs to be aware that the formation of induced tracks recorded in the  
215 mica detectors of the unknown samples, age standards and the dosimeter glasses also have  
216 Poisson distributions. This is why track counts of spontaneous and induced tracks for samples,  
217 standards and dosimeter glasses are taken into account for calculating age uncertainties (see  
218 age and error equations in Galbraith, 2005). In our sample set from the Bengal fan and the  
219 river samples a particular challenge is to deal with a large number of apatites that do not  
220 contain any (zero-track grains) or only very few (<4) spontaneous fission tracks. If a grain has  
221 zero, one, two or three spontaneous fission tracks it may either have a very young apparent  
222 cooling age or a very low U concentration, or both. Young low U concentration grains tend to

have large age uncertainties. This can result in apparent cooling age estimates that are younger than the depositional age without being affected by partial annealing. The true but unknown and poorly constrained cooling age of such apatite grains may well be older than the age of deposition of these grains,. In order to evaluate single grain ages of such grains we not only provide the single grain ages, but also the 95% confidence intervals in which most likely the true cooling age of each single grain lies (Galbraith, 2005). The 95% confidence intervals for each grain age were calculated with the Binomfit program of M. Brandon. In addition, for all samples central and minimum ages were calculated using the RadialPlotter program of Vermeesch (2009). The central age is an estimate of an average fission-track age of a grain-age distribution, which may be heavily over-dispersed, whereas the minimum age is an estimate of the youngest coherent grain-age population within a detrital grain-age distribution (Galbraith, 2005).

Given the relatively low closure temperature of the AFT thermochronometer (~110°C for F-OH apatite (e.g. Reiners and Brandon, 2006), and the ~60-110°C AFT partial annealing zone (PAZ) temperature range, depending on mineral chemistry and holding time within the PAZ, existing fission tracks may be progressively annealed after deposition (e.g. Reiners and Brandon, 2006). In the case of the Bengal fan most apatites are F-rich, a result already obtained by Corrigan and Crowley (1990).

#### *4. 2 Exhumation rate estimations*

As the main objective of this study was to estimate rates of exhumation from the detrital AFT data, we decided to use the minimum age approach (Galbraith, 2005 and references herein), instead of the more commonly used binomial peak-fitting approach, which was applied in previous studies on the Siwaliks Formation (van der Beek et al. 2006; Chirouze et al., 2013). For most samples this does not make a big difference, as in many cases the

minimum age and the first peak determined by binomial peak-fitting are identical or do overlap at the 95% confidence level. Nonetheless, applying the minimum age model avoids sample size (number of grains) bias to younger ages (Galbraith, 2005). Therefore, for the samples that fail the  $\chi^2$  homogeneity test and that have a considerable (>20%) dispersion of their single grain age distribution, the minimum age provides a more reliable estimate of the first coherent age population (Galbraith, 2005). The minimum age lag time can provide an estimate on the fastest exhumation rates in the source area, with the lag time being defined as the difference between the apparent AFT age and the depositional age (e.g. Bernet et al., 2006). The same calculation can be done with the central ages for an estimate on mean exhumation rates. In the absence of post-depositional partial annealing, the lag time integrates the time between cooling of the apatite below the fission-track closure temperature in the source rock, exhumation towards the surface, erosion, sediment transport in the fluvial system, and deposition in the Bengal fan. For the Himalaya, transport times can be considered as being negligible (Lupker et al., 2017), and the lag time is considered as a direct measurement of erosional and tectonic exhumation within the source area at the time of deposition. We use a 1D thermal advection model (Appendix D) to obtain first-order estimates of average exhumation rates from our AFT lag-time data.

## **5. Apatite fission-track results**

### *5.1. Bengal fan turbidites*

Twenty-three samples from 17.7 to 1153.4 m below sea floor and respectively from 0.3 to 17.2 Ma stratigraphic age were analysed (Table 1). The results show the typical wide range of non-reset detrital grain ages between 0.2 Ma and about 70 Ma with central ages ranging between 0.9 and 14 Ma and minimum ages between 1.7 and 12.1 Ma (Fig. 2). Most of the samples fail the  $\chi^2$  test and show large grain age dispersions of >30% (see Appendix B for the details of

every samples). For the four samples that do pass the  $\chi^2$  test only 30 or less grains could be dated. A total of nineteen samples have central ages equal or older than the depositional age at the 95% confidence level. Central and minimum AFT ages are also regularly older in deeper and stratigraphically older sediments (Fig. 2). For the site U1450, one sample displays both central and minimum ages younger than the modelled age of deposition. For the deeper site U1451, eight samples have their central and minimum ages younger than their deposition ages, of which six samples are within their 2-sigma error range overlapping with the depositional age (Table 1). The peculiar results of these samples are discussed below. For both sites U1450 and U1451, the difference between the central and the minimum ages of the Bengal fan samples is on average less than 1.5 Myr and for many samples both age estimates overlap at the 95% confidence level.

Radial plots and cumulative grain age plots with the single grain 95% age confidence intervals have been performed (Figs. 3 and 4 and Appendix B). Finally, the age-U concentration relationship indicates that many of the grains with <2 Ma apparent AFT cooling ages have U concentrations in the 10-100 ppm U range (Fig. 5).

## *5.2. Himalayan modern river sand apatite fission-track data*

New AFT ages of river sediments of the Brahmaputra, Siang, Sun Kosi, Daraundi Khola, Marsyandi, and Bothe Kosi rivers are shown in Table 2. Grain ages of the Himalayan river sands range between 0.2 Ma and about 48 Ma. The older, Eocene ages are found in the Siang and Marsyandi rivers only. All the eight Himalayan river samples fail the  $\chi^2$  test (Appendix C). Central ages of the Himalayan river sand samples vary between  $1.2 \pm 0.2$  Ma and  $4.6 \pm 0.5$  Ma and minimum ages range between  $0.66 \pm 0.66$  (Rangit River) to  $3.7 \pm 1$  Ma (Fig. 6 and Appendix B).

## 6. Discussion

Young AFT cooling ages are widely documented from *in situ* bedrock studies (e.g. Blythe et al., 2007; Thiede and Ehlers, 2013), which reinforce our findings. Below, we first detail and comment on the samples for which have AFT ages younger than the depositional ages (Table 1). We then give the implications of young AFT and short lag time ages for the long-term exhumation rates in the Ganga-Brahmaputra catchment, for the erosion processes providing young detrital apatites to the drainage system and finally its implications regarding tectonic/erosion/climate interactions over the last 13 Ma.

### 6.1 Interpreting apatite fission-track ages based on low track counts

The AFT age versus U concentration plot of the Bengal fan sediments shows that AFT cooling ages of <2 Ma are not restricted to grains with very low (<10 ppm) U concentrations. The same observation may be done from the detrital apatites carried by the modern Himalayan rivers (Fig. 5). Nonetheless, the interpretation of AFT ages based on low (<4) spontaneous tracks per grain, is difficult.

One could first argue that the low spontaneous track counts of the samples with younger AFT ages than their depositional age is related to post-depositional partial annealing because of reheating caused by burial heating and/or hydrothermal fluid flow. Given that 1) the sediments were collected from <1200 m below seafloor, and 2) the maximum depositional age is ~16 Ma (Fig. 2), partial annealing of fission-tracks in apatite would be highly unlikely if the basin geothermal gradient is not in excess of ~100°C/km. Present-day thermal gradients measured during IODP Expedition 354 are on the order of 40°C/km (France-Lanord et al., 2016), consistent with ocean basins of same age of 90–100 Ma and other values measured in the Bay of Bengal (Hasterok et al., 2011). For such a geothermal gradient, the 60–100°C AFT partial annealing zone is reached from burying depth of 1500 m, which is not the case for the

concerned samples (Table 1 and Fig. 2). In addition, the occurrence of smectite and the absence of illite rich smectite-illite mixed-layered clay minerals within the clay mineral fraction of the turbidites sampled for AFT analysis (France-Lanord et al., 2016), independently suggests that temperatures of partial annealing were never reached. Smectite starts to turn into illite at temperatures of 70-95°C (Lanson, 1995), which corresponds to the upper part of the AFT partial annealing zone (e.g. Reiners and Brandon, 2006). Therefore we have to consider another explanation for their young AFT ages.

Samples with only few apatite (<30 grains) may present central or minimum ages younger than the depositional age (table 1). Sample U1450A 110F is an example for this situation (Fig. 3) and only 26 single grain could be analysed with 19 grains with zero spontaneous tracks, and 6 with only 1 or 2 spontaneous tracks, leaving only 1 grain with >2 spontaneous tracks (Appendix B). An additional interesting observation is that the minimum age of this sample is older than the central age, being drawn up by the one older grain, with the highest U concentration (Fig. 3). The central and minimum ages of this sample have relatively large uncertainties. Less than 30 grains were also analysed for samples U1451A 74F4 and U1451B 51R2 generating AFT age uncertainties greater than those for samples with more grains counted (Fig. 3). Therefore, we do not consider those samples in the following.

At site U1451, more samples with minimum and/or central ages younger than the depositional age (negative lag times) can be observed especially for the deepest samples (Fig. 2 and Table 1). Sample U1451A 37F2, has central and minimum ages younger than the depositional age of  $6.53 \pm 0.3$  Ma. For this sample 74 grains were dated, but 32 of these grains (43%) have very low (<4) spontaneous track counts (see Appendix B), which skew the minimum and central ages to younger values, as grains with higher track counts of this sample result in ages older than the depositional age (Fig. 4). Therefore, we will not consider this sample in the following discussion and exclude these results in respect of our interpretation.

Samples U1451A 86F2, U1451B16 R1, U1451B 27R1, U1451B 37R2 and U1451B 45R1 all have minimum or central AFT ages that overlap with the 2-sigma error range with their depositional ages (Table 1). Sample U1451A 86F2 has ~20% of the 70 grains dated with <4 spontaneous tracks, sample U1451B 16R1 42% of 100 dated grains, sample U1451B 27R1 19% of 69 grains dated, sample U1451B 37R2 46% of 59 grains dated and sample U1451B 45R1 68% of 89 grains (Appendix B). The radial plot of U1451B 45R1 shows that higher U-concentration grains have younger apparent cooling ages (Fig. 4C). The lowermost sample U1451B 58R2W with a depositional age of  $17.2 \pm 0.5$  Ma and a 1046.89 m burial depth, has minimum and central ages that are considerably younger than the depositional age (e.g. negative minimum age lag times of  $8.2 \pm 5.1$  Myr), as shown in Table 1. For this sample only 32 grains could be dated of which 38% have low spontaneous track counts.

One can also note that from 550m in the U1451 site (Fig. 2), turbidite main granulometry is finer and composed of clayey silt instead of fine sands in the upper stratigraphic levels and in site U1450, making the sampling of apatite grain more difficult and less abundant. Therefore, the stratigraphically lowermost samples just show the importance of obtaining as many single grain ages as possible from high track density grains if available to get more tightly constrained age estimates.

Our analysis underlines that the AFT dating method reaches its detection limits when dealing with grains that have low spontaneous track counts and low U concentrations.

## *6. 2. Detrital Apatite fission-track signal and modern erosion in Himalaya*

The average AFT central age value is  $2.53 \pm 0.28$  Ma and  $2.9 \pm 0.39$  for the rivers draining respectively the Central and Eastern Himalaya, which are the rivers belonging to the Ganga or Brahmaputra catchment (Fig. 7). The river sediments, which were obviously collected much closer to their source areas than the Bengal fan sediments, provide a faithful representation of



the *in situ* bedrock AFT age distribution in the source (e.g. Thiede and Ehlers, 2013 and references therein), suggesting a very short transit and delivery time from the source to the sink. Such a short transit time is also reflected by the late Quaternary Bengal Fan AFT samples, the AFT central ages of which are very similar to the Himalayan rivers AFT ages discussed above (Table 2, Figs. 5-7) and suggests almost no transient storage in both the fluvial plain and delta.

Young *in situ* AFT ages (Burbank et al., 2003; Blythe et al., 2007; Whipple et al., 2016) are either found in zones close to and north of the sharp topographic transition (Fig. 1B) of the Greater Himalaya domain (Thiede and Ehlers, 2013 and references therein), or in the Namche Barwa and Nanga Parbat syntaxial antiforms (e.g. Zeitler et al., 2001; Seward and Burg, 2008). Although the exhumed areas are narrow, laterally discontinuous, and located on the southern side of the Himalaya, they provide the youngest apatite to the river system (Thiede and Ehlers and references therein). Seven out of eight rivers have central ages of 3 Ma or less (Table 2 and Fig. 7), for the rivers draining the sharp topographic transition and higher Himalayan relief. Therefore the influence of these areas is significant with respect to sediment input to the rivers. The dominance of apatite with about 2-3 Ma fission-track ages is enhanced because the formations north of the sharp topographic transition mainly consist of the apatite-richer Greater Himalayan Sequence (Robert et al., 2011). Focused exhumation of the steep Namche Barwa syntaxis, with young AFT cooling ages (0.7-1.1 Ma *in situ* AFT ages; Seward and Burg, 2008), is also significantly contributing to the Brahmaputra River (AFT minimum and central ages of respectively  $2.61 \pm 0.83$  Ma and  $3.05 \pm 0.39$  Ma) close to its confluence with the Ganges River.

The detrital AFT age value for the rivers are averaging different source areas, and the small average difference for rivers draining the Central and Eastern Himalaya strongly suggest a near impossibility to distinguish the provenance (Central or Eastern Himalaya) of detrital

apatite in the Bengal fan sediments (Fig. 7). Additional information, which would allow distinguishing different source rocks, would be needed. Nonetheless, in both cases, the apatites originate from areas with steep slopes of sharp relief, which are exhumed rapidly.

Exhumation rates are significantly correlated with high stream power and landslide erosion rates along steep slopes in the Namche Barwa massif (Larsen and Montgomery, 2012). Similarly, the high exhumation rates evidenced in central Himalaya by younger than 2 Ma *in situ* AFT ages (e.g. Robert et al., 2011) correlates with a sharp topographic relief displaying steep slopes close to a  $\sim 33^\circ$  threshold angle (Hodges et al., 2004) and strongly incised by river channels with a high stream power (Lavé and Avouac, 2001). Almost  $\sim 14\,000$  landslides induced by the 2015 Gorkha earthquake are located close and to the north of this physiographic transition between Higher and Lesser Himalaya domains and are characterized by slopes greater than  $35^\circ$  (e.g. Tsou et al., 2018). Therefore the exhumation of the youngest detrital AFT population found downward of these zones is controlled by a threshold hillslope-model of erosion, where landscape evolution is linked to landslide erosion, tectonic uplift, fluvial forcing and efficient sediment evacuation.

### *6.3. Long-term exhumation signal from apatite fission-track data*

The main observation drawn from the Bengal fan AFT data in this study is the occurrence of apatite with central AFT ages having lag times averaging  $2.26 \pm 1.6$  Myr) since the mid-Miocene (Table 1, Fig 7). These short lag times imply that some Himalayan source areas were rapidly exhumed at least at rates of 1 to 3 mm/yr, as estimated from a 1D thermal advection model for fluor apatite (Appendix D).

Previous studies in the proximal Siwalik foreland basin deposits of the Central Himalaya (van der Beek et al. 2006), and Eastern Himalaya (Coutand et al., 2016 and Chirouze et al., 2013) indicate AFT data ages that mainly range from 0.3 to 35 Ma. The

Bengal Fan and Siwalik data were acquired with a similar method. We compare below the central AFT ages already published in the Siwaliks with the Bengal Fan AFT central ages (as central and minimum ages overlap at 95% confidence level). For the last 6-7 Ma (older AFT data in the Siwaliks are subjected to partial annealing), the mean lag time for the Central and Eastern Siwaliks are respectively  $2.47 \pm 1.7$  Myr and  $2.13 \pm 1.44$  Myr while it is of  $2.19 \pm 1.6$  Myr from the Bengal Fan turbidites. These results are therefore very similar and overlap at  $2\sigma$  level, although the catchment basin of the Bengal Fan is much greater and may contain older sources than the ones of the Central and Eastern Siwalik domains (Fig. 7 and Tables 3 and 5). This suggests that sources have been rapidly exhumed in both central and eastern catchments from 6-7 Ma. Provenance analysis of the apatite should provide the litho-tectonic localisation of young apatite and how the exhumation varies in space and time, but this is not beyond the scope of this study. The lack of post depositional partial annealing for the Bengal Fan AFT data allows extending the record of exhumation back to 13 Ma. It shows that for the period 7-13 Ma, young apatite were also provided by the main Himalayan rivers, indicating that there has always been areas of rapid erosional exhumation, supplying detrital apatites to the fluvial system and delivering them to the paleo Ganges and/or Brahmaputra plains and finally to the Bengal Fan. The rate of such a rapid exhumation might not correspond to the same areas through time, but is relatively constant over the last 13 Ma. Another feature rising from this analysis is that the Siwalik foreland basin has been an overfilled basin since at least 13 Ma. Finally, the detrital apatite fission-track ages of the Bengal Fan turbidites display similar lag time characteristics to the AFT ages carried by present-day Himalayan rivers. Therefore, the processes described in the above section for the modern erosion in the Himalayan range could be extended in the past and we suggest that, over the last 13 Ma, apatite were mainly derived from areas of sharp relief, where river stream power was high and hill slopes close to the threshold angle.

#### 6.4. Detrital fission tracks and tectonic/erosion/climate interactions over the past 13 Ma

It has been suggested that erosion of the Himalaya is enhanced by the intense monsoonal rainfall (e.g. Burbank et al., 2003) and that an east-west climatic gradient involving higher amount of precipitation and higher erosion in the east than in the west (e.g. Bookhagen and Burbank, 2010) controls the tectonics of the thrust wedge (e.g. Chalaron et al., 1995). Neither an east/west regional or a temporal evolution of the exhumation is visible in the detrital AFT data of the modern Himalayan rivers, in the Bengal fan deposits or in the Neogene Siwaliks foreland basin deposits of the central and eastern Himalaya (Fig. 7).

Marked differences in precipitation and seasonality occurred within the Bengal fan catchment over the past 13 Ma as suggested by stable carbon and oxygen isotopic studies (e.g. Dettman et al., 2001), and they might have modified the erosion of the Himalaya and be recorded in the sedimentary flux of the Bengal Fan (Krishna et al., 2016). Although these climate/erosion relationships remain an active debate for the global Plio-Pleistocene (e.g. Herman et al., 2013; Schildgen et al., 2018 and references therein) or for the late Miocene (e.g. Clift et al., 2008), the erosion of the Himalaya has increased at the onset of the Plio-Pleistocene Northern Hemisphere cooling (Herman et al., 2013) or in the Late Miocene affected by an intensification of monsoon (e.g. Clift et al., 2008). Although the sedimentary flux from the 12 Ma long stable drainage system (Galy et al., 2010) seems to reflect these events (Krishna et al., 2016), the AFT data (Fig. 7) do not reveal any significant variation in erosion rate. We suggest that this difference is linked to a mixing of material coming from different domains affected by different erosion rate. In this study the minimum ages of the AFT reflect the domains of the most rapid exhumation. The absence of a climatic signal in these data agrees with the predictions of the threshold hillslope model (e.g. Larsen and Montgomery, 2012), which is less sensitive to climatic variations, as rainfall only affects

erosion through variations of the river profiles (e.g. Whipple and Tucker, 2002), which are buffered by variations of the stream power due to changes in the river width (e.g. Lague, 2013).

Therefore the detrital AFT data do not have the precision to trace the effect of climate-variability on exhumation rates on the <2 Myr timescale. In contrast, the persistence of detrital apatite with short AFT lag times in the Bengal fan sediments may be rather linked to the distribution of tectonically driven uplift on longer time-scales, and the morphology of the mountain belt. Given that exhumation within the main Himalayan orogen since at least 13 Ma propagated southward (Fig. 8) as suggested by A) the classical forward propagating thrust systems model of e.g. DeCelles et al., (2001 or Bollinger et al., (2006); and B) the  $\epsilon$ Nd studies performed in the Siwaliks of the Central Himalaya (e.g. Huyghe et al., 2001) and in the Bengal fan (Galy et al., 2010), the locus of rapid exhumation may have changed over time. Therefore, continuous rapid exhumation evidenced in the Bengal fan AFT data most likely reflects the underlying tectonic scheme driven by a permanent convergence between Asia and India and strong resulting uplift localized in limited areas such as the syntaxes or the hanging walls of crustal ramps.

## 7. Conclusions

Detrital AFT ages determined from turbidite deposits of the middle part of the Bengal fan provide a long-term record of Himalayan exhumation. Since at least 13 Ma, apatite grains with short minimum and central lag times (respectively  $1.55 \pm 3.13$  Myr and  $2.26 \pm 1.6$  Myr) were deposited in the Bengal fan. Apatite with such short lag times are also found in river sediments of the modern Ganges and Brahmaputra drainage system. Therefore, the lag time over the past 13 Ma and the modern lag time both support that temporary storage of detrital

apatite in the floodplains of the river drainage or in the delta are negligible and that exhumation rates have been consistently fast on the order of at least 1-3 km/Myr. Therefore, there have always been areas of fast erosion in the Himalayan range. Comparison of the AFT data of the Bengal Fan with those of the Central and Eastern proximal Neogene Himalayan foreland basin shows that both paleo Ganga and Brahmaputra catchments provided apatite with short lag time to the distal Bengal fan basin. Additional provenance analysis is needed to determine how such a fast exhumation varied in space and time.

The AFT data from the modern Himalayan erosion system show that apatites with short AFT lag times are derived from zones undergoing relatively rapid exhumation along the southern flank of the Himalaya. In these zones, the dominant processes of erosion are controlled by high stream power of the rivers that efficiently transport fluvial sediments and by a threshold angle triggering landslides and limiting the slope of the hills. Therefore, by analogy with the modern erosion processes in the Himalayan range, we suggest that over the past 13 Ma apatite were mainly derived from areas of sharp relief, where river stream power was high and hill slopes close to the threshold angle. Consequently, the maximum exhumation rate provided by the Bengal fan apatite were not strongly affected by climatic variations related by the onset of the Plio-Pleistocene Northern Hemisphere cooling or by the reported intensity changes of the Indian Monsoon. The maximum exhumation rates provided by the minimum and central ages of the AFT of the Bengal fan are characteristic of the tectonic processes at the Ma scale resolution.

## **Acknowledgments**

This work was supported by IODP France and Labex Osug@2020 grants and the CNRS. We thank Melanie Balvay, Francis Coeur and Francois Senebier of the Geo-Thermochronology (GTC) platform at ISTERre, Université Grenoble Alpes, for help with sample preparation for apatite fission-track analysis. The manuscript benefited from thorough and constructive comments by P. Copeland, R. Thiede and A.A.G. Webb. We also thank D. Burbank and P. DeCelles for improving an earlier version of the manuscript.

## References

- Abrahami, R., van der Beek, P., Huyghe, P., Hardwick, E., and Carcaillet, J., 2016. Decoupling of long-term exhumation and short-term erosion rates in the Sikkim Himalaya, Earth and Planetary Science Letters, 433, 76-88, 10.1016/j.epsl.2015.10.039.
- Bernet, M., van der Beek, P., Pik, R., Huyghe, P., Mugnier, J.-L., Labrin, E., Szulc, A., 2006. Miocene to Recent exhumation of the central Himalaya determined from combined detrital zircon fission-track and U/Pb analysis of Siwalik sediments, western Nepal. Basin Research 18, 393-412, <https://doi.org/10.1111/j.1365-2117.2006.00303.x>
- Blythe, A.E., Burbank, D.W., Carter, A., Schmidt, K., Putkonen, J., 2007. Plio-Quaternary exhumation history of the central Nepalese Himalaya: 1. Apatite and zircon fission track and apatite [U-Th]/He analyses. Tectonics 26, n/a-n/a, <https://doi.org/10.1029/2006tc001990>
- Bollinger, L., Henry, P., Avouac, J., 2006. Mountain building in the Nepal Himalaya: Thermal and kinematic model. Earth and Planetary Science Letters 244, 58-71, <https://doi.org/10.1016/j.epsl.2006.01.045>
- Bookhagen, B., Burbank, D.W. 2010. Toward a complete Himalayan hydrological budget: spatiotemporal distribution of snowmelt and rainfall and their impact on river discharge. J. Geophys. Res. Earth Surf. 115:F03019. doi:10.1029 /2009JF001426.

- 545 Burbank, D.W., Blythe, A.E., Putkonen, J., Pratt-Sitaula, B., Gabet, E., Oskin, M., Barros, A., Ojha,  
546 T.P., 2003. Decoupling of erosion and precipitation in the Himalayas. *Nature* 426, 652-655,  
547 <https://doi.org/10.1038/nature02187>
- 548 Cervený, P.F., Naeser, N.D., Zeitler, P.K., Naeser, C.W., Johnson, N.M., 1988. History of Uplift and  
549 Relief of the Himalaya During the Past 18 Million Years: Evidence from Fission-Track Ages of  
550 Detrital Zircons from Sandstones of the Siwalik Group, in: Kleinspehn, K.L., Paola, C. (Eds.),  
551 *New Perspectives in Basin Analysis*. Springer New York, New York, NY, pp. 43-61.
- 552 Chalaron, E., Mugnier, J.L., Mascle, G., 1995. Control on thrust tectonics in the Himalayan foothills: a  
553 view from a numerical model. *Tectonophysics* 248, 139-163, [https://doi.org/10.1016/0040-](https://doi.org/10.1016/0040-1951(94)00281-d)  
554 [1951\(94\)00281-d](https://doi.org/10.1016/0040-1951(94)00281-d)
- 555 Chirouze, F., Huyghe, P., van der Beek, P., Chauvel, C., Chakraborty, T., Dupont-Nivet, G., Bernet, M.,  
556 2013. Tectonics, exhumation, and drainage evolution of the eastern Himalaya since 13 Ma from  
557 detrital geochemistry and thermochronology, Kameng River Section, Arunachal Pradesh.  
558 *Geological Society of America Bulletin* 125, 523-538, <https://doi.org/10.1130/b30697.1>
- 559 Clift, P.D., Hodges, K.V., Heslop, D., Hannigan, R., Van Long, H., Calves, G., 2008. Correlation of  
560 Himalayan exhumation rates and Asian monsoon intensity. *Nature Geoscience* 1, 875-880,  
561 <https://doi.org/10.1038/ngeo351>
- 562 Copeland, P., and Harrison, T.M., 1990. Episodic rapid uplift in the Himalaya revealed by <sup>40</sup>Ar/<sup>39</sup>Ar  
563 analysis of detrital K-feldspar and muscovite, Bengal fan, *Geology*, 18, 354-357, 10.1130/0091-  
564 7613(1990)018<0354:eruith>2.3.co;2
- 565 Corrigan, J.D., Crowley, K., 1990. Fission-Track Analysis of Detrital Apatites from Sites 717 and 718,  
566 Leg 116, Central Indian Ocean.
- 567 Coutand, I., Barrier, L., Govin, G., Grujic, D., Hoorn, C., Dupont-Nivet, G. and Najman, Y. 2016. Late  
568 Miocene- Pleistocene evolution of India-Eurasia convergence partitioning between the Bhutan  
569 Himalaya and the hillong Plateau: New evidences from foreland basin deposits along the  
570 Dungsam Chu section, eastern Bhutan, *Tectonics*, 35, 2963-2994, 10.1002/2016tc004258



571 DeCelles, P.G., Robinson, D.M., Quade, J., Ojha, T.P., Garziane, C.N., Copeland, P., Upreti, B.N.,  
572 2001. Stratigraphy, structure, and tectonic evolution of the Himalayan fold-thrust belt in western  
573 Nepal. *Tectonics* 20, 487-509, [10.1029/2000tc001226](https://doi.org/10.1029/2000tc001226)

574 Dettman, D.L., Kohn, M.J., Quade, J., Ryerson, F.J., Ojha, T.P., Hamidullah, S., 2001. Seasonal stable  
575 isotope evidence for a strong Asian monsoon throughout the past 10.7 m.y. *Geology* 29, 31-34,  
576 [https://doi.org/10.1130/0091-7613\(2001\)029%3C0031:SSIEFA%3E2.0.CO;2](https://doi.org/10.1130/0091-7613(2001)029%3C0031:SSIEFA%3E2.0.CO;2)

577 Elliott, J.R., Jolivet, R., González, P.J., Avouac, J.P., Hollingsworth, J., Searle, M.P., Stevens, V.L.,  
578 2016. Himalayan megathrust geometry and relation to topography revealed by the Gorkha  
579 earthquake. *Nature Geoscience* 9, 174-180, <https://doi.org/10.1038/ngeo2623>

580 France-Lanord, C., Spiess, V., Klaus, A., Schwenk, T., Scientists, t.E., 2016. Bengal Fan, in: France-  
581 Lanord, C., Spiess, V., Klaus, A., Schwenk, T. (Eds.), *Proceedings of the International Ocean*  
582 *Discovery Program*. International Ocean Discovery Program, College Station, TX.

583 Galbraith, R.F., 2005. *Statistics for Fission Track Analysis*. CRC Press, p. -219.

584 Galy, A., France-Lanord, C., Derry, L.A., 1996. The Late Oligocene-Early Miocene Himalayan belt  
585 Constraints deduced from isotopic compositions of Early Miocene turbidites in the Bengal Fan.  
586 *Tectonophysics* 260, 109-118, [https://doi.org/10.1016/0040-1951\(96\)00079-0](https://doi.org/10.1016/0040-1951(96)00079-0)

587 Galy, V., France-Lanord, C., Peucker-Ehrenbrink, B., Huyghe, P., 2010. Sr–Nd–Os evidence for a  
588 stable erosion regime in the Himalaya during the past 12Myr. *Earth and Planetary Science*  
589 *Letters* 290, 474-480, <https://doi.org/10.1016/j.epsl.2010.01.004>

590 Garzanti, E., Andò, S., France-Lanord, C., Vezzoli, G., Censi, P., Galy, V., Najman, Y., 2010.  
591 Mineralogical and chemical variability of fluvial sediments1. Bedload sand (Ganga–  
592 Brahmaputra, Bangladesh). *Earth and Planetary Science Letters* 299, 368-381,  
593 [10.1016/j.epsl.2010.09.017](https://doi.org/10.1016/j.epsl.2010.09.017)

594 Gemignani, L., van der Beek, P., Braun, J., Naman, Y., Bernet, M., Garzanti, E. and Wijbrans, J.R.,  
595 2018. Downstream evolution of the thermochronologic age signal in the Brahmaputra catchment

596 (eastern Himalaya): Implications for the detrital record of erosion. *Earth and Planetary Science*  
597 *Letters* 499, 48-61, doi.org/10.1016/j.epsl.2018.07.019

598 Godin, L., Grujic, D., Law, R.D., Searle, M.P., 2006. Channel flow, ductile extrusion and exhumation  
599 in continental collision zones: an introduction. Geological Society, London, Special Publications  
600 268, 1,

601 Hasterok, D., Chapman, D.S., and Davis, E.E., 2011. Oceanic heat flow: impli- cations for global heat  
602 loss. *Earth and Planetary Science Letters*, 311(3– 4):386–395.  
603 <http://dx.doi.org/10.1016/j.epsl.2011.09.044>

604 Herman, F. , Seward, D., Valla, P.G., Carter, A., Kohn, B., Willett, S.D. and Ehlers, T.A., 2013.  
605 Worldwide acceleration of mountain erosion under a cooling climate, *Nature*, 504, 423-426,  
606 10.1038/nature12877.

607 Hodges, K.V., Wobus, C., Ruhl, K., Schildgen, T., Whipple, K., 2004. Quaternary deformation, river  
608 steepening, and heavy precipitation at the front of the Higher Himalayan ranges. *Earth and*  
609 *Planetary Science Letters* 220, 379-389, 10.1016/s0012-821x(04)00063-9

610 Hu, X., Garzanti, E., Moore, T. and Raffi, I, 2015. Direct stratigraphic dating of India-Asia collision  
611 onset at the Selandian (middle Paleocene,  $59 \pm 1$  Ma, *Geology*, 43, 859-862, 10.1130/g36872.1.

612 Huyghe, P., Galy, A., Mugnier, J.-L., France-Lanord, C., 2001. Propagation of the thrust system and  
613 erosion in the Lesser Himalaya: Geochemical and sedimentological evidence. *Geology* 29, 1007-  
614 1010, [https://doi.org/10.1130/0091-7613\(2001\)029%3C1007:POTSA%3E2.0.CO;2](https://doi.org/10.1130/0091-7613(2001)029%3C1007:POTSA%3E2.0.CO;2)

615 Krishna, K. S., M. Ismaiel, M., Srinivas, K., Gopala Rao, D., Mishra, J. and Saha, D., 2016. Sediment  
616 pathways and emergence of Himalayan source material in the Bay of Bengal *Current Science*,  
617 110, 3, 363-372, doi: 10.18520/cs/v110/i3/363-372.

618 Lague, D., 2013. The stream power river incision model: evidence, theory and beyond. *Earth Surface*  
619 *Processes and Landforms* 39, 38-61, <https://doi.org/10.1002/esp.3462>

620 Larsen, I.J., Montgomery, D.R., 2012. Landslide erosion coupled to tectonics and river incision. *Nature*  
621 *Geoscience* 5, 468, <https://doi.org/10.1038/ngeo1479>

622 Lavé, J., Avouac, J.P., 2001. Fluvial incision and tectonic uplift across the Himalayas of central Nepal.  
623 *Journal of Geophysical Research: Solid Earth* 106, 26561-26591,  
624 <https://doi.org/10.1029/2001jb000359>

625 Lupker, M., Lavé, J., France-Lanord, C., Christl, M., Bourlès, D., Carcaillet, J., Maden, C., Wieler, R.,  
626 Rahman, M., Bezbaruah, D., Xiaohan, L., 2017.  $^{10}\text{Be}$  systematics in the Tsangpo-Brahmaputra  
627 catchment: the cosmogenic nuclide legacy of the eastern Himalayan syntaxis. *Earth Surface*  
628 *Dynamics* 5, 429-449, 10.5194/esurf-5-429-2017

629 Mugnier, J.-L., and Huyghe, P., 2006. Ganges basin geometry records a pre-15 Ma isostatic rebound of  
630 Himalaya. *Geology* 34, <https://doi.org/10.1130/g22089.1>

631 Najman, Y., Bickle, M., BouDagher-Fadel, M., Carter, A., Garzanti, E., Paul, M., Wijbrans, J., Willett,  
632 E., Oliver, G., Parrish, R., Akhter, S.H., Allen, R., Ando, S., Chisty, E., Reisberg, L., Vezzoli, G.,  
633 2008. The Paleogene record of Himalayan erosion: Bengal Basin, Bangladesh. *Earth and*  
634 *Planetary Science Letters* 273, 1-14, <https://doi.org/10.1016/j.epsl.2008.04.028>

635 Reiners, P.W., Brandon, M.T., 2006. USING THERMOCHRONOLOGY TO UNDERSTAND  
636 OROGENIC EROSION. *Annual Review of Earth and Planetary Sciences* 34, 419-466,  
637 10.1146/annurev.earth.34.031405.125202

638 Reilly, B.T., 2018, Deciphering Quaternary geomagnetic, glacial, and depositional histories using  
639 paleomagnetism in tandem with other chronostratigraphic and sedimentological approaches,  
640 Ph.D. Thesis, Oregon State University, Corvallis, OR, 97331, USA

641 Robert, X., van der Beek, P., Braun, J., Perry, C., Mugnier, J.-L., 2011. Control of detachment geometry  
642 on lateral variations in exhumation rates in the Himalaya: Insights from low-temperature  
643 thermochronology and numerical modeling. *Journal of Geophysical Research* 116,  
644 <https://doi.org/10.1029/2010jb007893>

645 Schildgen, T.F., van der Beek, P.A., Sinclair, H.D. and Thiede, R.C., 2018. Spacial correlation bias in  
646 late-Cenozoic erosion history derived from thermochronology, *Nature*, 559, 89-93, doi.  
647 org/10.1038/s41586-018-0260-6

648 Seward, D., and Burg, J.-P., 2008. Growth of the Namche Barwa Syntaxis and associated evolution of  
649 the Tsangpo Gorge: Constraints from structural and thermochronological data. *Tectonophysics*  
650 451, 282-289, <https://doi.org/10.1016/j.tecto.2007.11.057>

651 Szulc, A.G., Najman, Y., Sinclair, H.D., Pringle, M., Bickle, M., Chapman, H., Garzanti, E., Andò, S.,  
652 Huyghe, P., Mugnier, J.L., Ojha, T., DeCelles, P., 2006. Tectonic evolution of the Himalaya  
653 constrained by detrital 40Ar-39Ar, Sm-Nd and petrographic data from the Siwalik foreland basin  
654 succession, SW Nepal. *Basin Research* 18, 375-391, 10.1111/j.1365-2117.2006.00307.x

655 Thiede, R.C., Ehlers, T.A., 2013. Large spatial and temporal variations in Himalayan denudation. *Earth*  
656 and Planetary Science Letters 371-372, 278-293, <https://doi.org/10.1016/j.epsl.2013.03.004>

657 Tsou, C.-Y., Chigira, M., Higaki, D., Sato, G., Yagi, H., Sato, H.P., Wakai, A., Dangol, V., Amatya,  
658 S.C., Yatagai, A., 2018. Topographic and geologic controls on landslides induced by the 2015  
659 Gorkha earthquake and its aftershocks: an example from the Trishuli Valley, central Nepal.  
660 *Landslides* 15, 953-965,

661 van der Beek, P., Robert, X., Mugnier, J.-L., Bernet, M., Huyghe, P., Labrin, E., 2006. Late Miocene –  
662 Recent exhumation of the central Himalaya and recycling in the foreland basin assessed by  
663 apatite fission-track thermochronology of Siwalik sediments, Nepal. *Basin Research* 18, 413-  
664 434, <https://doi.org/10.1111/j.1365-2117.2006.00305.x>

665 Vermeesch, P., 2009, RadialPlotter: A Java application for fission track, luminescence and other radial  
666 plots. *Radiation Measurements*, 44, 409-410.

667 Webb, A.A.G, Guo, H., Clift, P.D., Husson, L., Müller, T., Costantino, D., Yin, A., Xu, Z., Cao, H., and  
668 Wang, Q., 2017, The Himalaya in 3D: Slab dynamics controlled mountain building and  
669 monsoon intensification, *Lithosphere*, 9, 637–651. doi: <https://doi.org/10.1130/L636.1>

- Whipple, K.X., Shirzaei, M., Hodges, K.V., Ramon Arrowsmith, J., 2016. Active shortening within the Himalayan orogenic wedge implied by the 2015 Gorkha earthquake. *Nature Geoscience* 9, 711, <https://doi.org/10.1038/ngeo2797>
- Whipple, K.X., Tucker, G.E., 2002. Implications of sediment-flux-dependent river incision models for landscape evolution. *Journal of Geophysical Research: Solid Earth* 107, ETG 3-1-ETG 3-20, 10.1029/2000JB000044
- Yin, A., Harrison, T.M., Murphy, M.A., Grove, M., Nie, S., Ryerson, F.J., Feng, W.X., Le, C.Z., 1999. Tertiary deformation history of southeastern and southwestern Tibet during the Indo-Asian collision. *Geological Society of America Bulletin* 111, 1644– 1664, <https://doi.org/10.1130/0016-7606>.
- Zeitler, P.K., Koons, P.O., Bishop, M.P., Chamberlain, C.P., Craw, D., Edwards, M.A., Hamidullah, S., Jan, M.Q., Khan, M.A., Khattak, M.U.K., Kidd, W.S.F., Mackie, R.L., Meltzer, A.S., Park, S.K., Pecher, A., Poage, M.A., Sarker, G., Schneider, D.A., Seeber, L., Shroder, J.F., 2001. Crustal reworking at Nanga Parbat, Pakistan: Metamorphic consequences of thermal-mechanical coupling facilitated by erosion. *Tectonics* 20, 712-728, <https://doi.org/10.1029/2000tc001243>

## Figure captions

Figure 1:

A) The Ganga-Brahmaputra catchment of the Bengal Fan (from Galy et al. 2010) - B: Bhopal; C: Kolkata; D: Delhi; K: Kathmandu; NBS: Namche Barwa Syntaxis; THB: Tran-Himalayan Batholiths. River names are those cited in the text and are indicated by the following symbols.  $\alpha$ : SunKoshi,  $\beta$ : Brahmaputra;  $\chi$ : Subansiri;  $\delta$ : Rangit,  $\epsilon$ : Kameng,  $\phi$ : Marsyandi and Daraundi,  $\gamma$ : Bhote Kosi,  $\lambda$ : Karnali;  $\eta$ : Siang;  $\mu$ : Dibang;  $\rho$ : Rapti. Location of sampling is displayed by stars for apatites.

B): Sketch of the inferred structural elements of the Indo-Asia collision zone controlling localized rapid exhumation rates (orange, purple and red lines refer respectively to the 110°C isotherm related to the AFT closure temperature, to the brittle/ductile transition and to the 750°C isotherm below which partial melt starts). In the brittle regime : 1) the Main Himalayan Thrust (MHT) is affected by a crustal ramp (e.g. Elliot et al., 2016) that migrated during the evolution of the range and delineates duplexes (e.g. De Celles et al., 1998); 2) internal shortening (Whipple et al., 2016) including 3) out-of-sequence thrust (Hodges et al., 2004); In the ductile regime (thin lines): distributed shearing (horizontal arrows) and vertical flattening define a channel flow (ChF) (Godin et al., 2013) with a fast exhumation zone (4) at its frontal edge and/or (5) a lateral extrusion in the syntaxes (e.g. Zeitler et al., 2001).

Figure 2: Variation of the AFT central ages (blue diamond) and AFT minimum ages (red square) versus depth for the two drilling sites U1450 and U1451 (Bengal Fan, 8°N). Horizontal bars correspond to 2 $\sigma$  uncertainty. Red line represents the age model based on the magnetostratigraphic model of Reilly (2018) for the <1.9 Ma deposits and on polynomial extrapolation between shipboard and post-cruise biostratigraphic constraints based on nannofossil zones (France Lanord et al., 2016). The minimum age curve (grey dotted line) is established from the youngest fauna considering that older fauna in turbidite horizons could be reworking by the turbiditic current.

Figure 3: A) Cumulative AFT age plots, organized from youngest to oldest grains of selected samples showing the 95% age confidence intervals. Samples U1450A 24HG and U1450A 110F with respectively 100 and less than 30 counted grains are shown for comparison of the robustness of AFT ages; B) Apatite fission-track age radial plots of corresponding Bengal fan samples, showing central and minimum ages determined with RadialPlotter (Vermeesch, 2009). Radial plots and cumulative age plots of all samples are available in the Appendix B.

Figure 4: Radial plots of samples U1450A 6 7 8F (minimum and AFT central ages older than depositional age), U1451A 37F2 (minimum and AFT central ages younger than depositional age) and U1451B 45R1 (minimum and AFT central ages that overlap with the 2-sigma error range with its depositional age) are shown for comparison. Radial plot of sample U1451B 45R1, displays a trend of apatite with younger cooling ages and higher U concentrations.

Figure 5: A) Single grain AFT age versus U concentration plot of detrital apatite grains of sample series U1450A and U1451A. B) Plot for apatite with fission-track cooling ages <2Ma). C) Single grain AFT age versus U concentration plot of detrital apatite grains from modern Himalayan river sediments. The red dotted line correspond(s) to 10 ppm U concentration below which grains are considered to have a poor U content.

Figure 6: AFT age radial plots of the new Himalaya river samples presented in this study, showing central and minimum ages determined with RadialPlotter (Vermeesch, 2009).

Figure 7: Comparison between Bengal Fan, Siwaliks and Himalayan rivers AFT central ages. Bengal Fan AFT data are represented by blue diamonds, Siwalik AFT data from Central Himalaya (Van der Beek et al., 2006) by squares and Siwalik AFT data from Eastern Himalaya (Chirouze et al., 2013, Coutand et al., 2016) by triangles. Yellow squares and triangles represent AFT central ages of Himalayan rivers belonging, respectively, to the Ganga and Brahmaputra rivers.

Figure 8: Relationships between sharp topographic transition in Himalaya, exhumation short AFT lag time and transport toward the proximal and distal Bengal Fan foreland basins. When the 110°C exhumation path of apatite crystals (green line), reaches the topography, erosion occurs and material containing apatite is shed to the river system (blue line and arrows) and finally to the Bengal Fan. Green circles indicate the FT central lag time (in Myr) of detrital apatites in the rivers running in the proximal foreland basin and in the Bengal fan distal basin;

green squares indicate the *in situ* age range of the apatite provided by the steepest slopes. Three sketches are drawn from the available AFT data: modern Himalaya, 6-7 Ma Himalaya, 12-13 Ma Himalaya.

A) sketch of the Bengal fan U1451 drill hole (from France-Lanord et al. 2016) recording short AFT lag times since 13 Ma. For caption of the drill hole lithology, see Figure 2.

B) modern Himalayan sketch with sharp topographic transition above the ramp system and in the Namche Barwa syntaxis (NB). Recent AFT of the Bengal Fan and AFT of Himalayan rivers are from this paper. *In situ* AFT ages are from Burbank et al. (2003) and Blythe et al. (2007) above the Himalayan ramp system. *In situ* AFT ages are from Seward and Burg (2008) for the Namche Barwa syntaxis.

C) sketch of the persistence of very steep mountain zones related to rapid exhumation zone in Himalaya from 6-7 Ma to the present-day, as suggested by the AFT of the < 6-7 Ma Siwalik and Bengal Fan sedimentary records (van der Beck et al., 2006; Chirouze et al., 2013; Coutand et al., 2016 and this study); D) sketch of the persistence of very steep mountain zones related to fast exhumation zone in Himalaya from 7 to 13 Ma (as suggested by the Bengal fan sedimentary record, this study). No indication is given for the paleo-Himalayan rivers as AFT of the Siwalik proximal basin are reset.

## Tables

Table 1. Bengal fan detrital apatite fission-track data and central age lag-time estimates for samples from the IODP 345 sites 1450 and 1451

Table 2. Central and eastern Himalayan river detrital apatite fission-track data and sample locations

## Supplementary material:



771 Appendix A: Details of composite samples of the Bengal Fan  
772 Appendix B: Bengal fan data set - Apatite fission-track single grain age data, Apatite fission-  
773 track radial plots and grain age 95% confidence interval plots  
774 Appendix C: Himalayan rivers data set - Apatite fission-track single grain age data and Apatite  
775 fission-track radial plots  
776 Appendix D: Lag time to exhumation rate relationship determined with the 1D thermal  
777 advection model Age2Edot of Brandon (see Ehlers et al. 2005) for F-apatites.  
778  
779

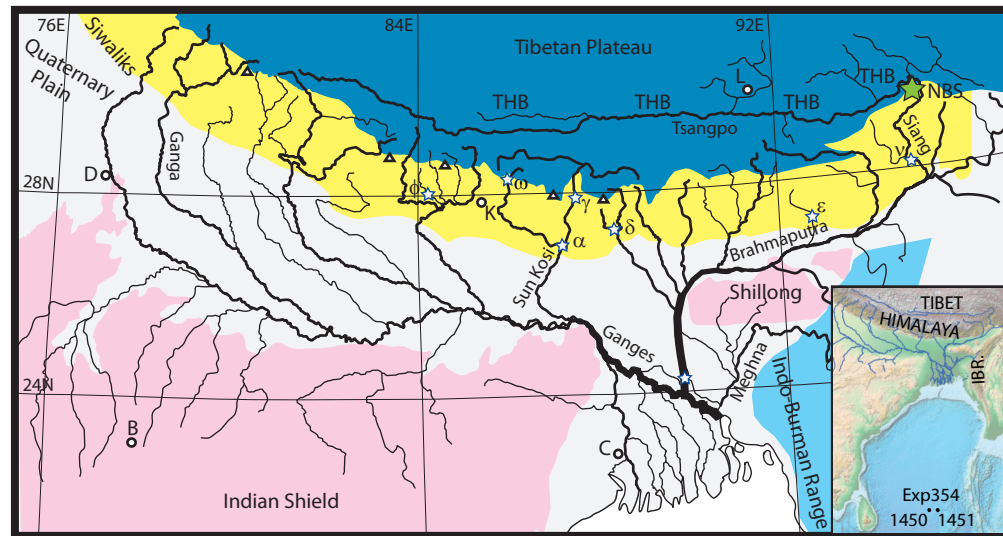


Figure 1a

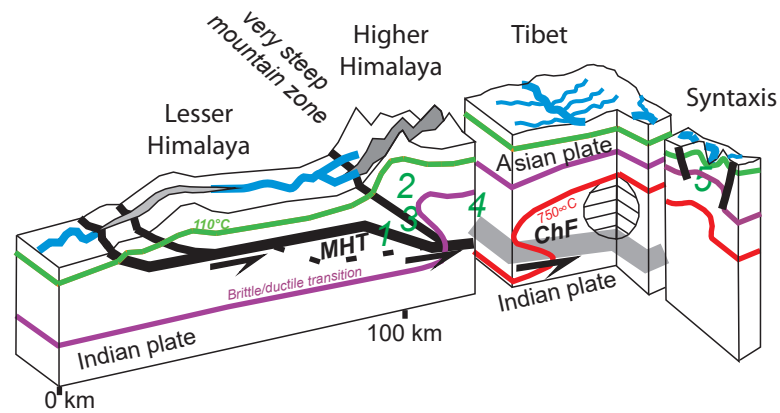
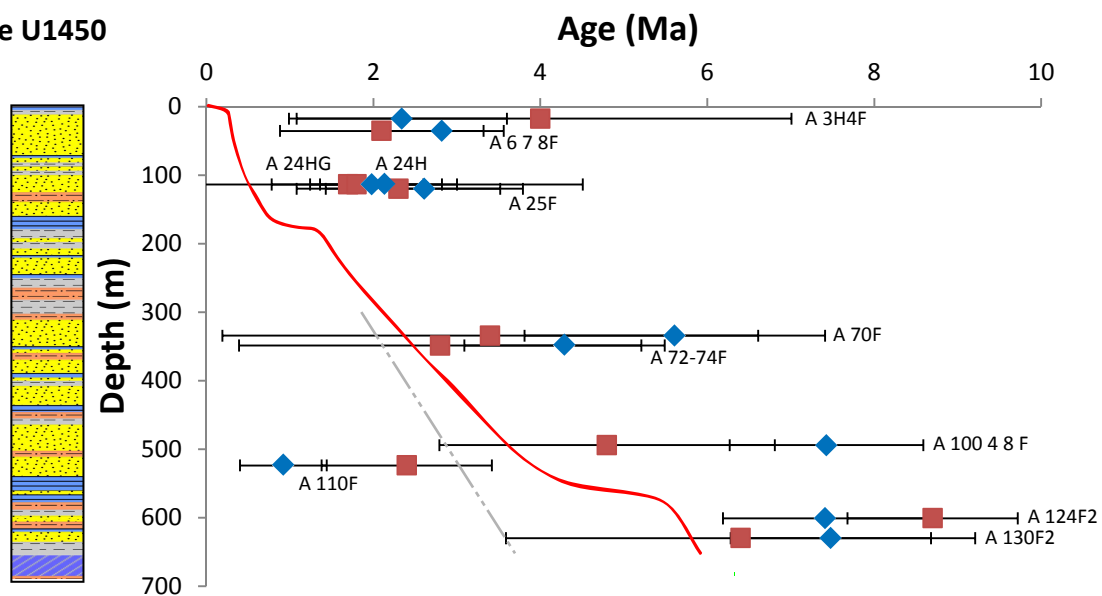
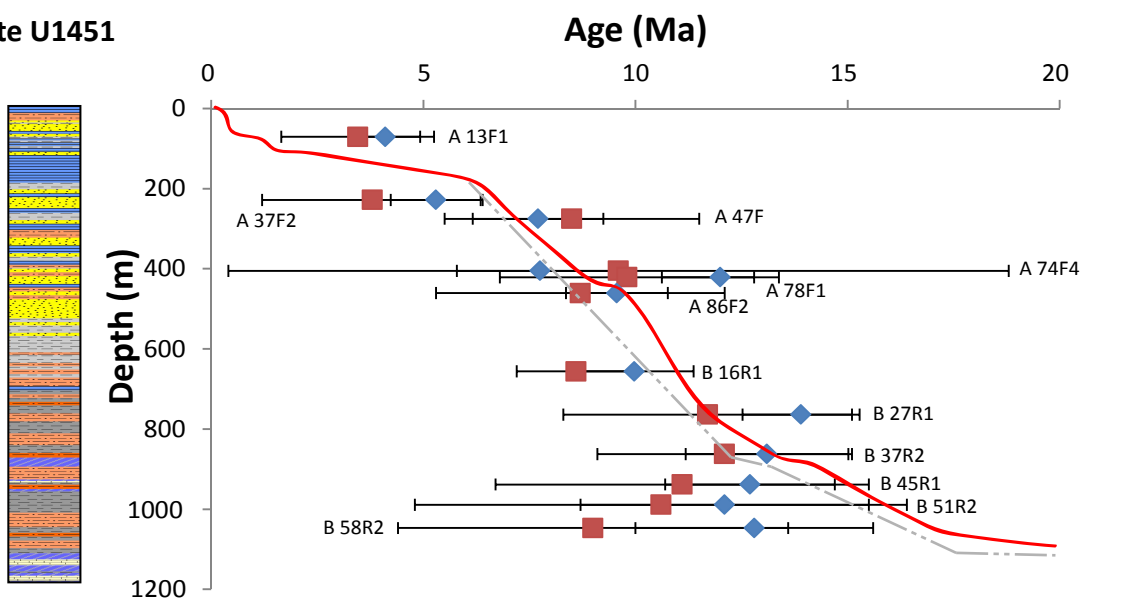










Figure 1b





## Site U1450



## Site U1451



-  Clay
-  Claystone
-  Silt
-  Siltstone
-  Sand
-  Calcareous clay
-  Calcareous claystone
-  Limestone

-  AFT Minimum age
-  AFT Central age
-  Age Model
-  Minimum depositional age

**Figure 2**

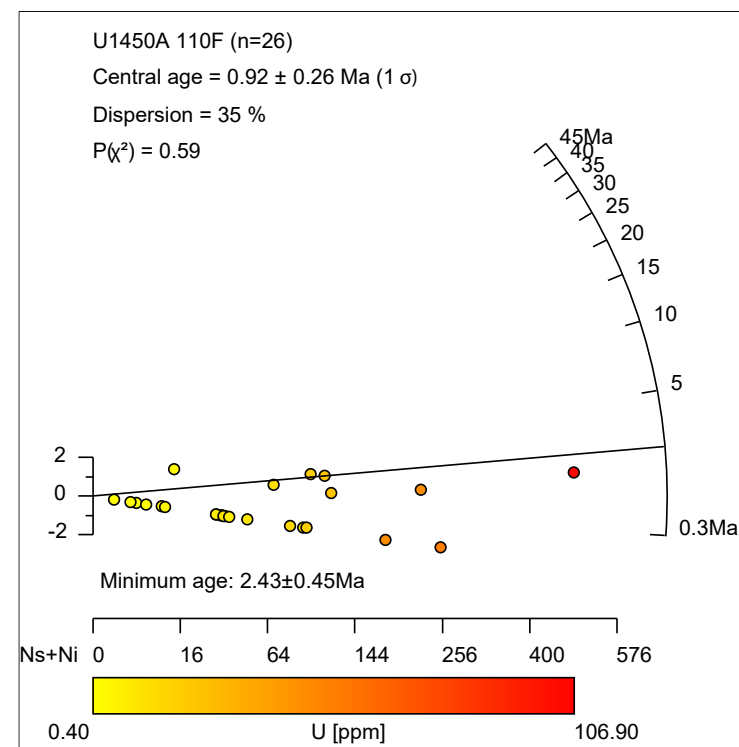
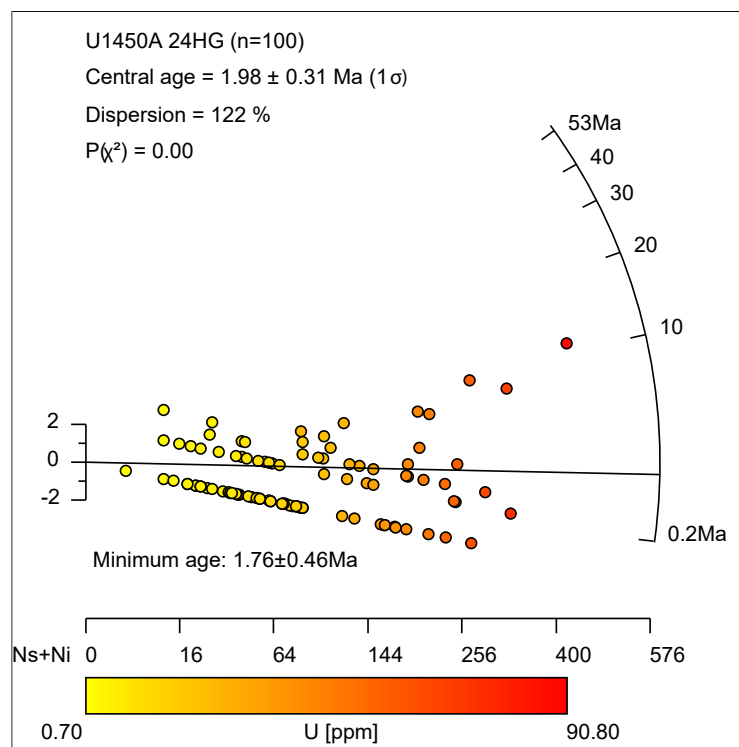
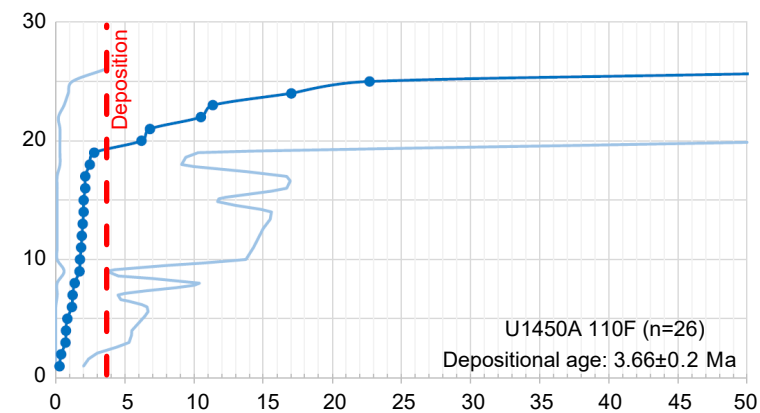
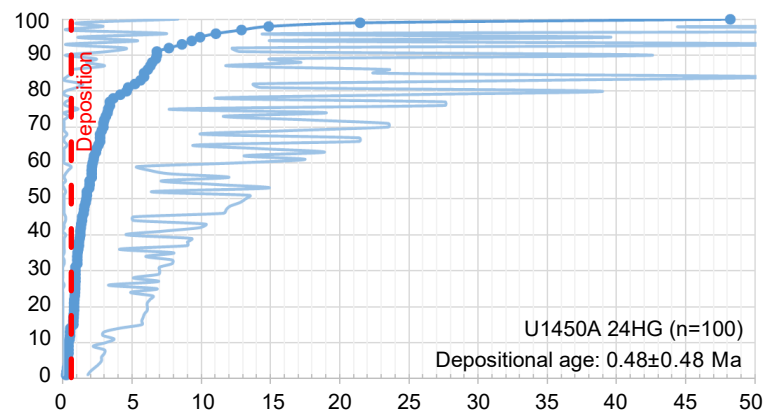
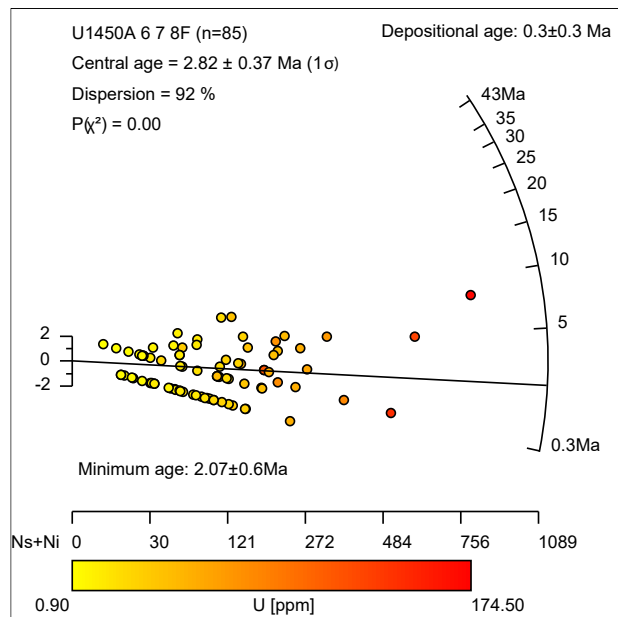
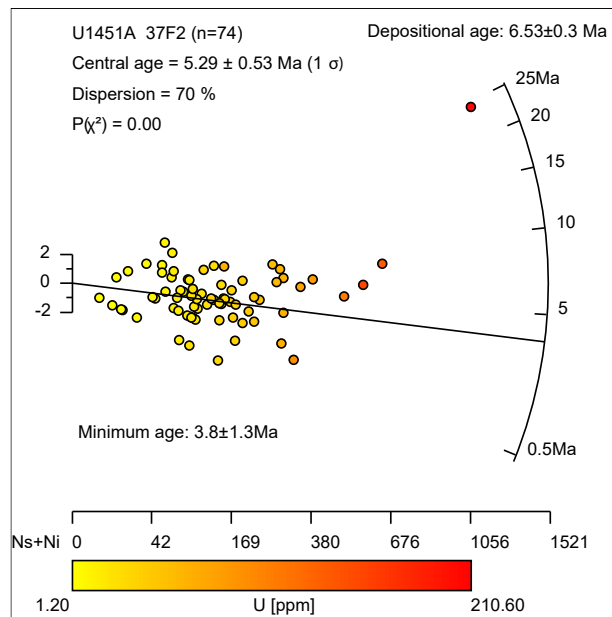


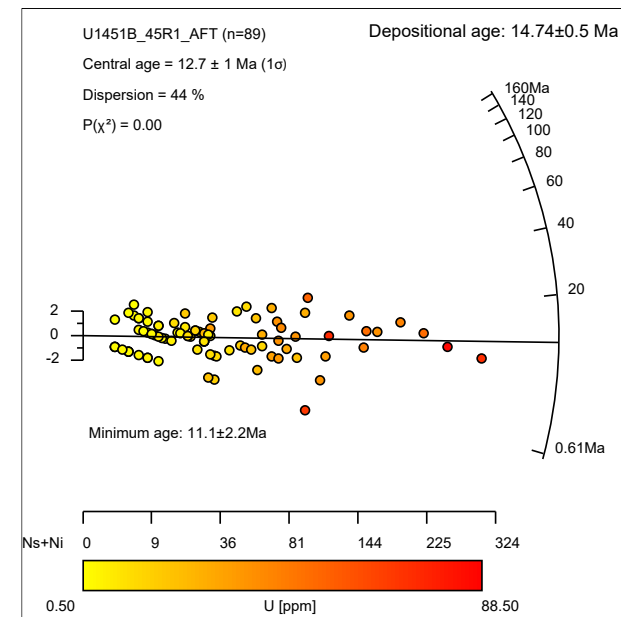
Figure 3



(a)



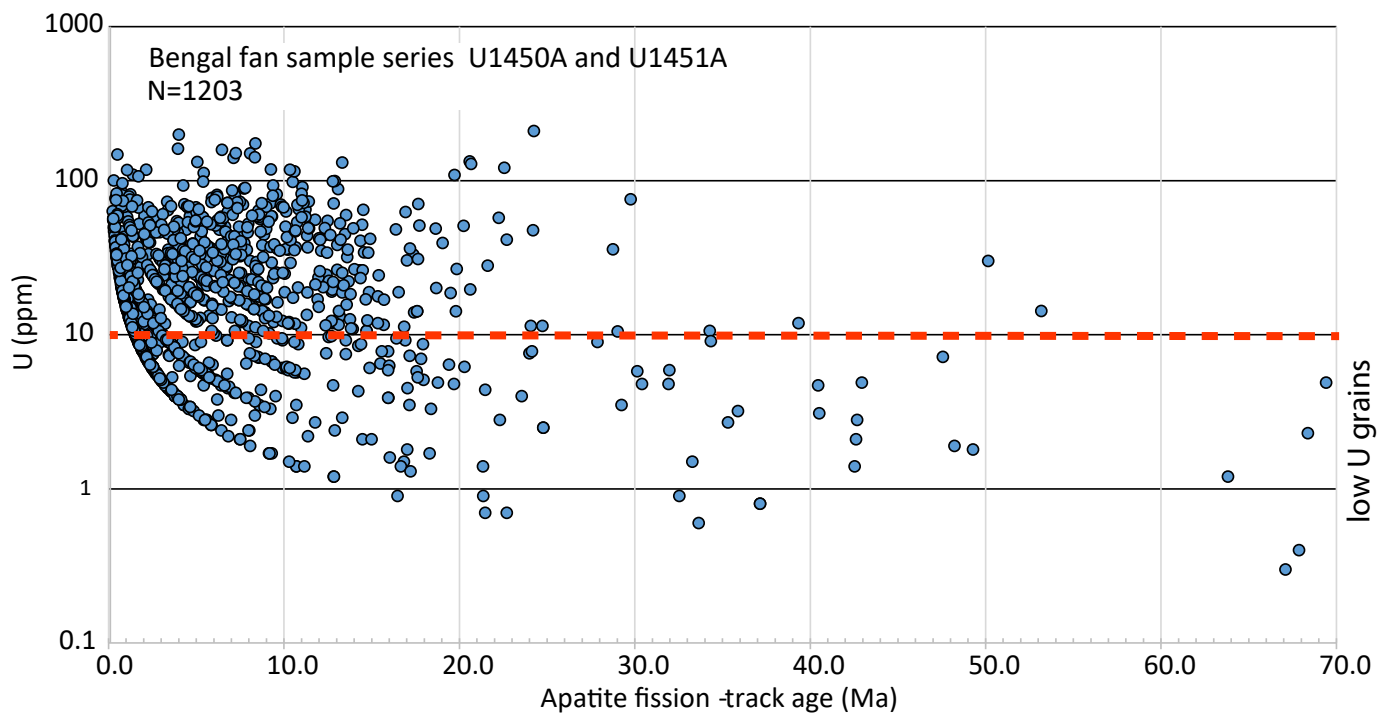
(b)



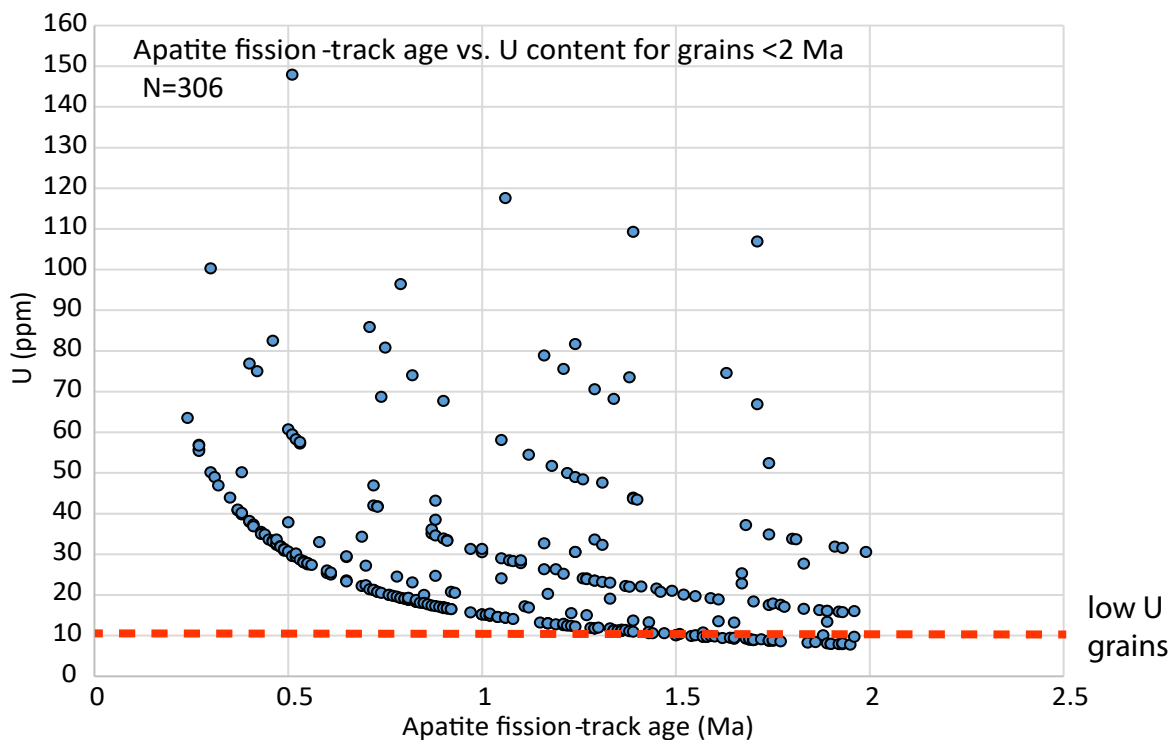
(c)

Figure 4

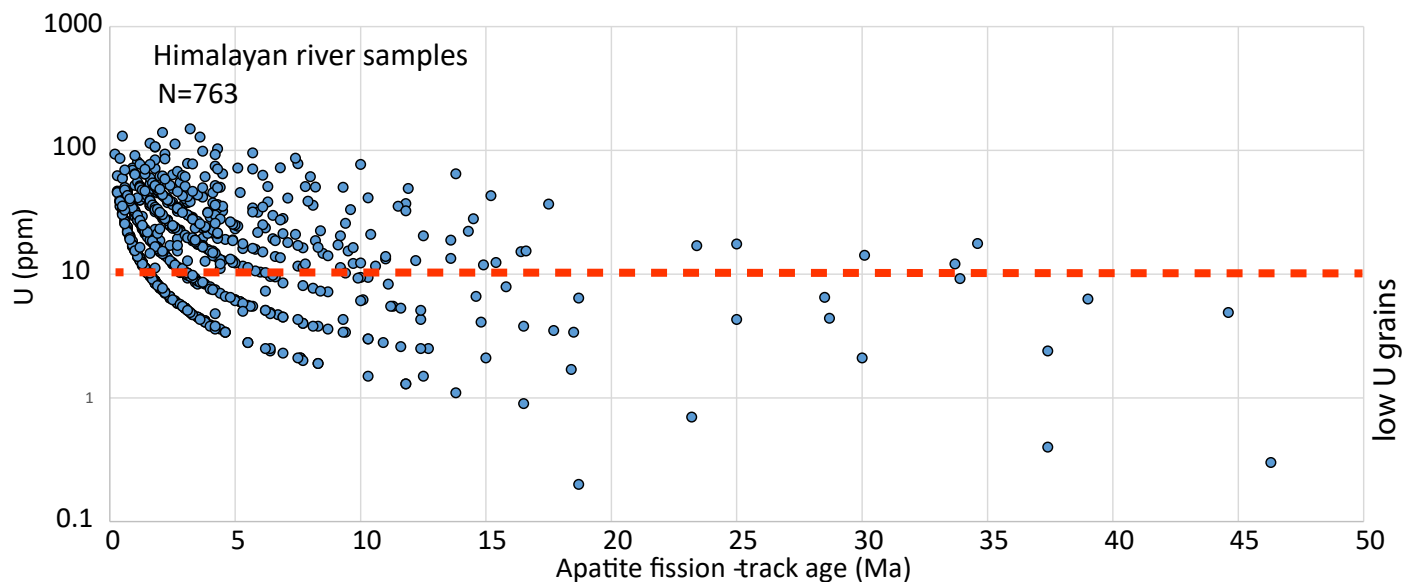
A) Apatite fission-track age vs. U content



B) Apatite fission-track age vs. U content for grains <2 Ma



C) Himalayan river samples



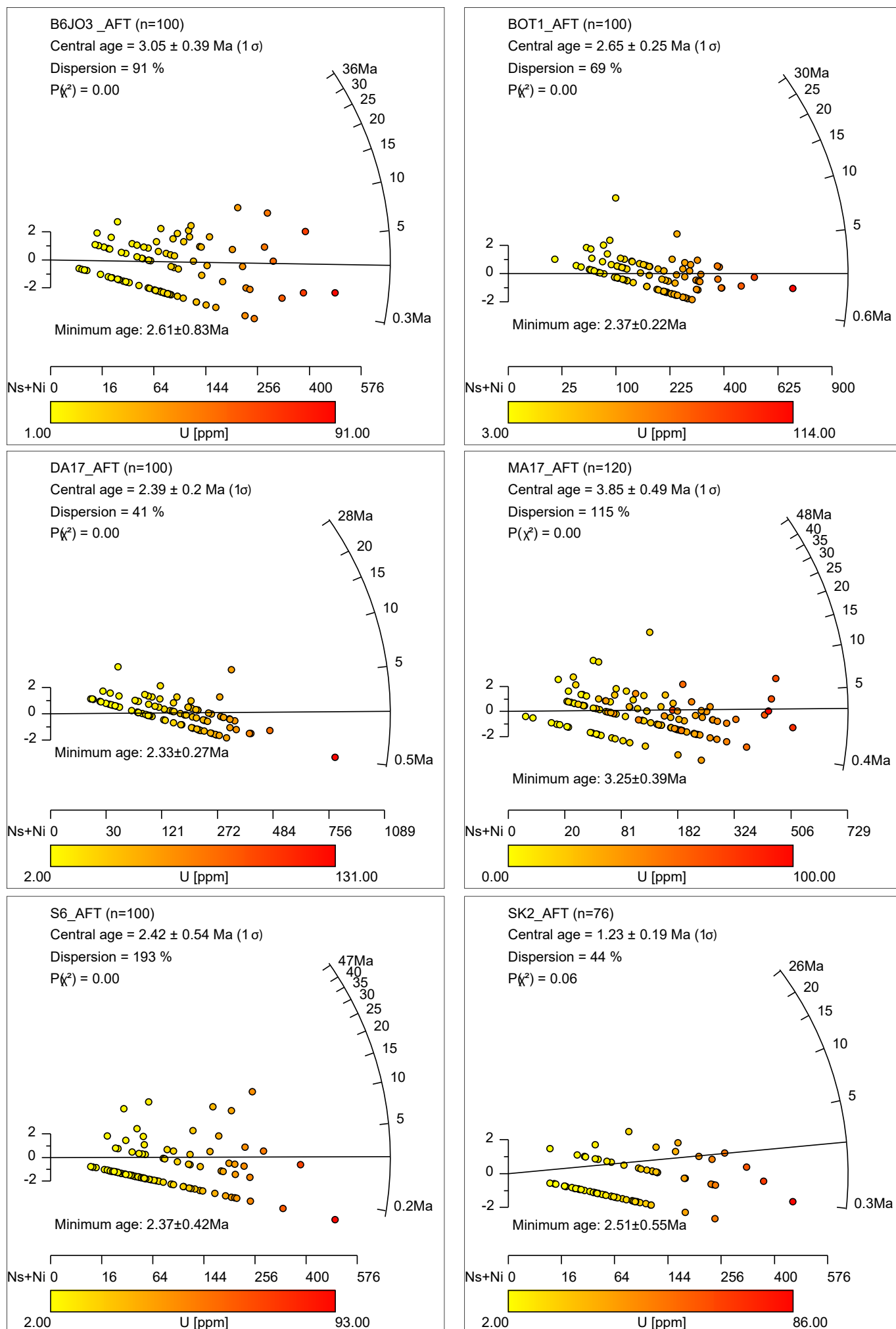


Fig. 6

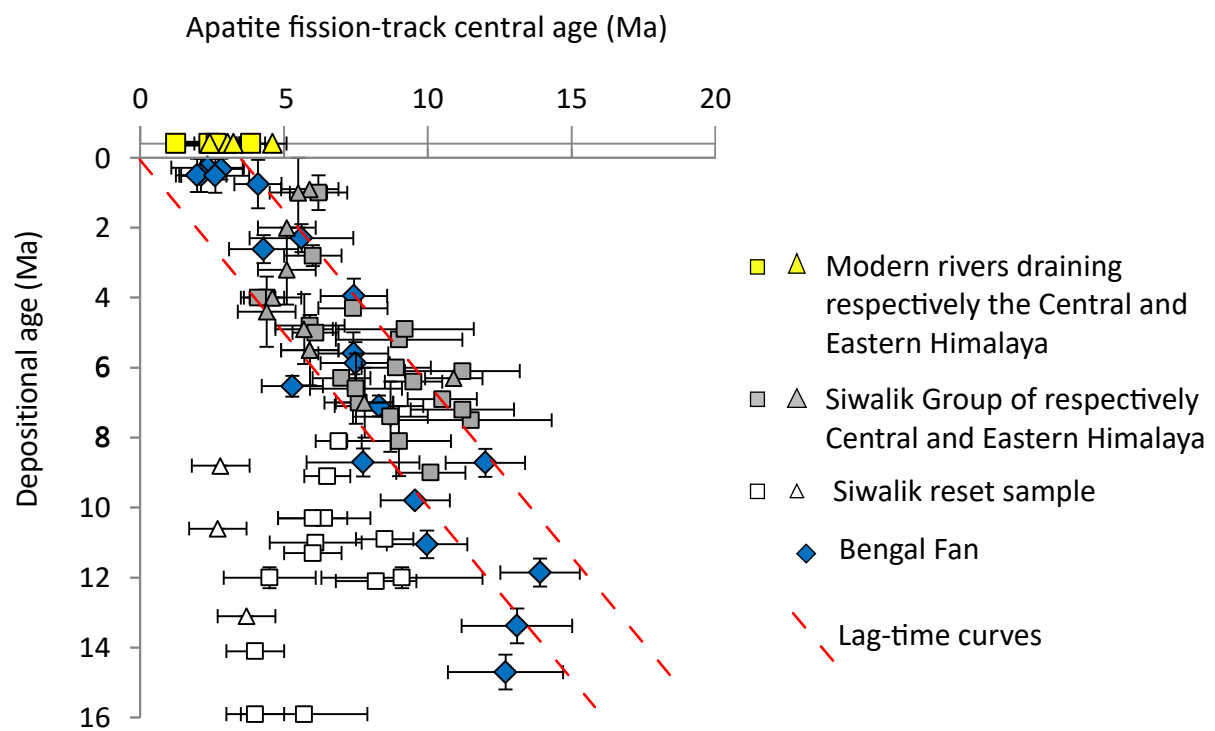


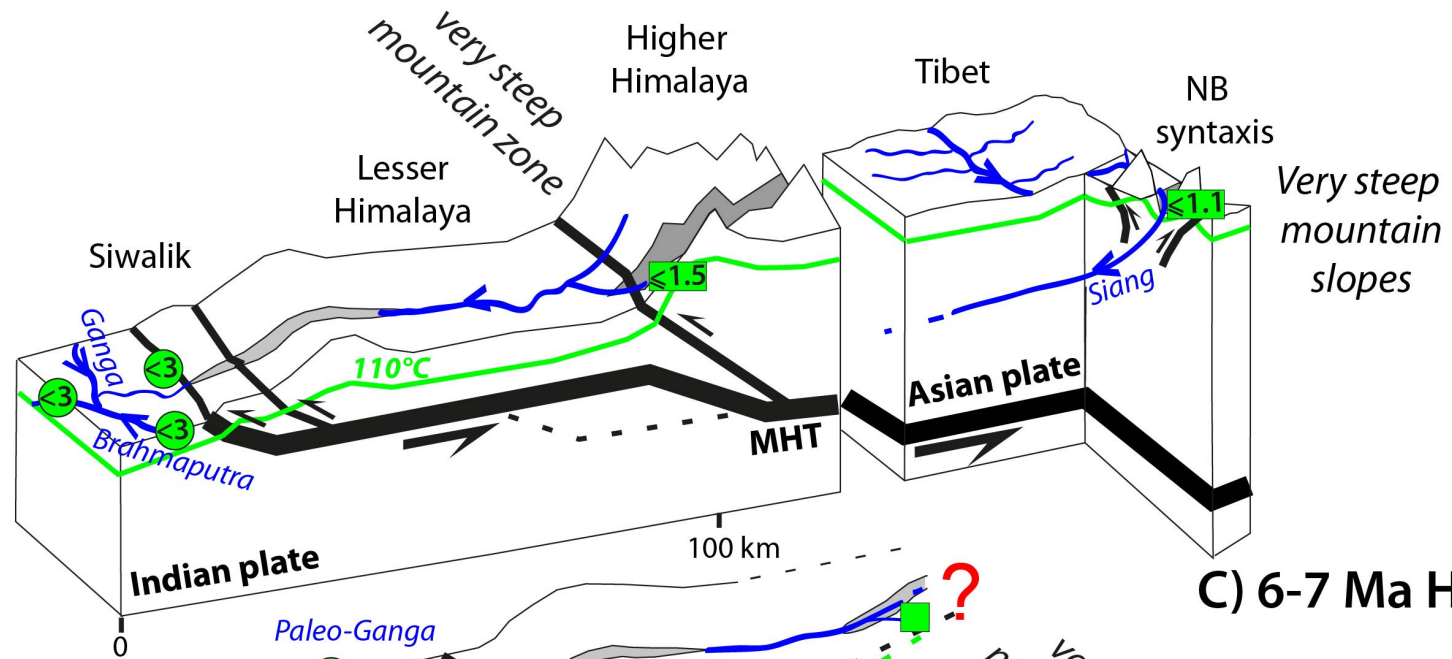
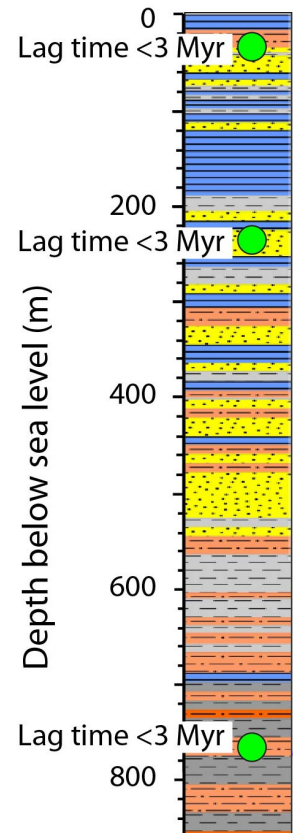
Figure 7



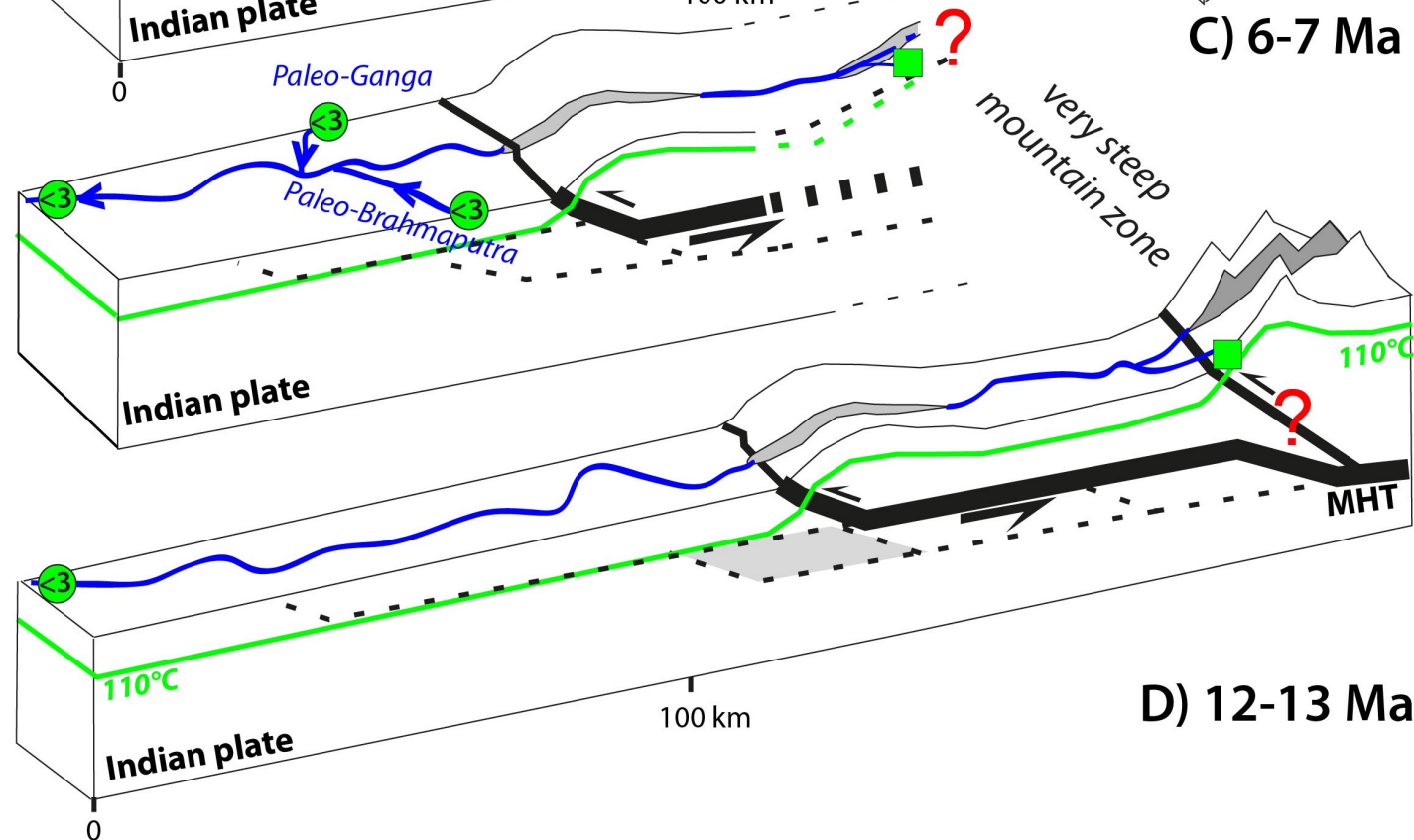
## A) Bengal Fan

## B) Modern Himalaya

### Site U1451



### C) 6-7 Ma Himalaya



### D) 12-13 Ma Himalaya

Figure 8